Regular Article

PHYSICAL CHEMISTRY RESEARCH
Published by the
Iranian Chemical Society
www.physchemres.org
info@physchemres.org

Phys. Chem. Res., Vol. 8, No. 4, 671-687, December 2020
DOI: 10.22036/pcr.2020.227546.1763

Experimental and Computational Investigations on the Molecular Structure, Vibrational Spectra, Electronic Properties, FMO and MEP Analyses of 4,6-Bis(4-Fluorophenyl)-5,6-dihydropyrimidin-2(1H)-one: A DFT Insight

S.S. Pathade[a,*] and B.S. Jagdale[b]

[a]*Department of Chemistry, Maharaja Sayajirao Gaikwad Arts, Science and Commerce College Malegaon, (Affiliated to SP Pune University) Nashik-423 105, India*

[b]*Department of Chemistry, Arts, Science and Commerce College, Manmad, (Affiliated to SP Pune University) Nashik-423 104, India*

(Received 19 April 2020, Accepted 10 July 2020)

In the present work, 4,6-bis(4-fluorophenyl)-5,6-dihydropyrimidin-2(1*H*)-one was synthesized by condensation of (2*E*)-1,3-bis(4-fluorophenyl)prop-2-en-1-one with urea in a basic medium. The synthesized compound was characterized using FT-IR and ^{1}H NMR spectroscopic techniques. To determine the molecular structure of the synthesized molecule some quantum chemical calculations were carried out by density functional theory (DFT) at the B3LYP/6-311++G(d,p) level in gas phase, water and CCl_4 solvents using Gaussian-03 package. The optimized geometrical parameters, thermochemical parameters and global reactivity descriptors were computed. The frontier molecular orbital (FMO) and molecular electrostatic potential (MEP) analyses were also performed to explore the reactivity of title molecule at the same level of theory. The vibrational frequencies of the title molecule were analysed and compared with the corresponding experimental data. The results show fair correlation between the calculated frequencies in gas phase and experimental frequencies. The effect of water and CCl_4 solvents on vibrational frequencies and global chemical reactivity descriptors were also examined. The results show that polar solvent water decreased the carbonyl stretching frequency significantly, while other frequencies in water and CCl_4 are slightly different than those in gas phase. In solvents, no significant change was observed on energy gap (ΔE) and global reactivity descriptors of the title molecule.

Keywords: FT-IR, B3LYP, Quantum chemical calculations, Gaussian

INTTRODUCTION

Chalcones (1,3-diarylprop-2-en-1-ones) are important precursors for the synthesis of many heterocyclic compounds such as pyrazolines, pyrimidines, isoxazoles, thiazines, flavones, benzodiazepines, *etc.* Most of these heterocyclic compounds are biologically active and are widely used in the life saving medicines. Pyrimidine is one of the prominent heterocyclic compound containing two nitrogen atoms at positions 1 and 3 in a six-member ring. Pyrimidine nucleus is an essential component in natural products like nucleic acids and vitamin B1. They also have remarkable pharmaceutical importance. Many pyrimidine derivatives have been found to have a broad spectrum of biological activities such as anti-inflammatory [1], antihypertensive [2], anticancer [3], antimalarial [4], antitubercular [5], antiviral [6] and antitumor [7,8]. Figure 1 shows some symbolic examples of pyrimidine derivatives as therapeutic agent. Given such vital properties of pyrimidine derivatives, organic and medicinal chemists are taking considerable synthetic efforts to construct these scaffolds by employing a new captivating strategy.

In recent decades, computational chemistry has become a promising tool beside experimental chemistry. The quantum chemical calculations using density functional

*Corresponding author. E-mail: sandip.pathade@yahoo.com

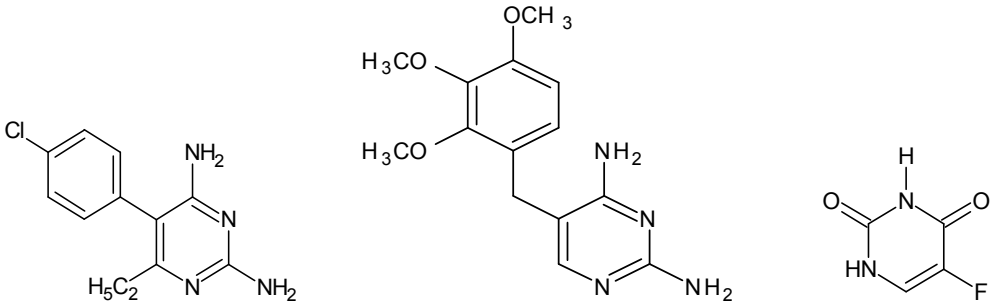

Pyrimethamine Trimethoprim 5-Fluorouracil

Fig. 1. Examples of pyrimidine derivatives as the therapeutic agents.

theory (DFT) play a significant role in exploring the chemical reactivity and physical properties of organic compounds. Computational investigations also help chemists make predictions before running the actual experiments, so that they can be better prepared for making observations.

Many studies have been reported in literature for synthesis of pyrimidines and theoretical investigations of compounds by using DFT method. The synthesis of a series of certain polymethoxy pyrimidine derivatives and thiazolopyrimidines was reported by Rostom *et al.* They characterized the synthesized compounds by IR and ^{1}H NMR spectral data and screened these compounds for their in-vitro anticancer and antimicrobial activity. They found that most of the compounds possess a significant antitumor activities [9]. The synthesis, characterization and anti-mycobacterial evaluation of hydroxy and nitro substituted pyrimidine derivatives from corresponding chalcones were reported by Trivedi *et al.* [10]. Umaa and co-workers reported the synthesis and characterization of substituted pyrimidines from chalcones on cyclisation with guanidine hydrochloride. The chalcones were prepared from the substituted acetophenones and aromatic aldehydes. They characterized the synthesized compounds by physical and spectral characterisation methods for establishment of the structures [11]. A series of dihydropyrimidinone derivatives were synthesized in good yields by Claisen Schmidt reaction of acetophenones with substituted aldehydes in the presence of sodium hydroxide in water-ethanol mixture followed by the condensation reaction of chalcones with urea [12].

Yokota and co-workers were synthesized novel 2-aminobenzo[4,5]thieno[3,2-d]pyrimidine-5,5-dioxides and reported their computational analysis by DFT with the B3LYP hybrid functional and 6-311G(d,p) basis set [13]. The N,N′-dipyridoxyl(1,2-diaminocyclohexane) Schiff-base ligand and its square complexes were synthesized by Beyramabadi *et al.* They also reported the geometry optimization of the synthesized compounds and their vibrational frequency calculation using the DFT method [14]. Santiago Aparicio reported a systematic computational study on flavonoids. He analysed the selected flavonoids by DFT through a systematic B3LYP/6-311++G** computational level with the aim of understanding the molecular factors that determine their structural and energetic properties in gas phase [15]. DFT studies and vibrational spectra of 2-bromoethyl-4-nitroanisole were reported by Arivazhagan *et al.* They computed the vibrational spectra by HF method at 6-31+G(d,p) level and DFT method at standard B3LYP/6-31+G(d,p) level. The computed spectra were compared with experimental FTIR spectrum and they found that the vibrations obtain from DFT method are in good agreement with experimental data [16]. Govindarasu *et al.* calculated the vibrational wavenumbers of N-(2,4-dinitrophenyl)-l-alanine methyl ester by DFT method with B3LYP and M06-2X/6-31G(d,p) levels of theory. The natural bond orbital (NBO) analysis has also been carried out to analyse the effects of intramolecular charge transfer, intramolecular and hyperconjugative interactions on the geometries. In

addition, they also investigated the frontier molecular orbitals, molecular electrostatic potential and thermodynamic properties of studied molecule [17]. Quantum mechanical calculations and spectroscopic investigations, such as FT-IR, FT-Raman and UV, molecular orbital, NBO and MEP analyses of 4-[5-(4-methylphenyl)-3-(trifluoromethyl)-1H-pyrazol-1-yl] benzene-1-sulfonamide using DFT method with B3LYP/6-311G(d,p) and 6-311++G(d,p) basis sets were performed by Govindasamy *et al.* [18]. The vibrational spectra of the organic molecules were calculated from the optimized geometry by employing Becke three-parameter with Lee-Yang-Parr (B3LYP) functional of DFT, and the wavenumbers computed were compared with experimental data [19-21]. Many studies have discussed the experimental and theoretical investigations of compounds by using DFT method. The DFT exploration provided an in-depth understanding of the reactivity and several molecular properties of the compounds studied [22-25].

In the present study, we report the synthesis and DFT based computational investigation of the electronic and structural properties of 4,6-bis(4-fluorophenyl)-5,6-dihydropyrimidin-2(1H)-one molecule. The comparison is performed between vibrational spectra computed in gas, water and CCl_4 with experimental FT-IR spectrum of the synthesized compound.

EXPERIMENTAL

All the chemicals required were obtained from commercial source (AR grade with purity > 99%) and used without further purification. Melting point of the compound was determined in open capillary tube and is uncorrected. The IR spectra was recorded on Shimadzu FT-IR spectrometer using potassium bromide pellets. ^{1}H NMR was determined on Bruker Avance II 500 MHz spectrometer using $CDCl_3$ as solvent and TMS as an internal standard. The reaction was monitored by thin layer chromatography (TLC, Merck) using aluminium sheets coated with silica gel using n-hexane and ethyl acetate as an eluent.

Synthesis of Chalcone (3)

Equimolar mixture of 4-fluoro acetophenone 1 (0.01 mol) and 4-fluoro benzaldehyde 2 (0.01 mol) in ethanol (15 ml) catalysed by 10% NaOH (10 ml) was stirred together at room temperature for 16 h. Then, the reaction mixture was poured into crushed ice and acidified with dilute HCl. The solid product (chalcone) obtained was filtered, washed with water, dried and recrystallized from ethanol.

Synthesis of 4,6-Bis(4-fluorophenyl)-5,6-dihydropyrimidin-2(1H)-one (4)

The solution of chalcone (0.002 mol) and urea (0.002 mol) in ethanolic sodium hydroxide (15 ml) was refluxed for 6 h. The progress of reaction was monitored by TLC. After completion of the reaction, the mixture was cooled to room temperature and poured into crushed ice. The solid obtained was filtered, washed, dried and recrystallized in ethanol to obtain pure title compound (4). The reaction path is shown in Scheme 1, and the characterization data of synthesized compound (4) are given below.

4,6-Bis(4-fluorophenyl)-5,6-dihydropyrimidin-2(1H)-one (4). Yeild: 90%, light yellow solid, m.p.: 124-126 °C. Experimental FT-IR spectrum is shown in Fig. 2. FT-IR (KBr, in cm^{-1}): 3337 (N-H str), 1678 (C=O str), 1589 (C=N str), 3074 (Ar-H str), 1523 (aro. C=C str), 1156 (Ar-F str). ^{1}H NMR (500 MHz, $CDCl_3$, in δ): 7.79-7.65 (m, 2H), 7.39-7.22 (m, 2H), 7.19-7.09 (m, 4H), 5.16 (s, 1H), 3.92 (dd, 1H), 2.76 (dd, 1H), 2.16 (dd, 1H).

Computational Details

All the computational calculations were performed in gas, water and CCl_4 phase by using Gaussian-03(W) package. In order to analyze the theoretical parameters of the compound, geometry was optimized by DFT method with B3LYP level at 6-311++G(d,p) basis set [26-28]. The optimized structure of compound was used for the frequency calculation. For a good agreement between a theoretical and experimental data the calculated frequencies were scaled using the Pulay scaled quantum mechanical force field methodology. The electronic properties, thermochemical parameters, HOMO-LUMO and MEP of title compound are also investigated by employing same level of theory.

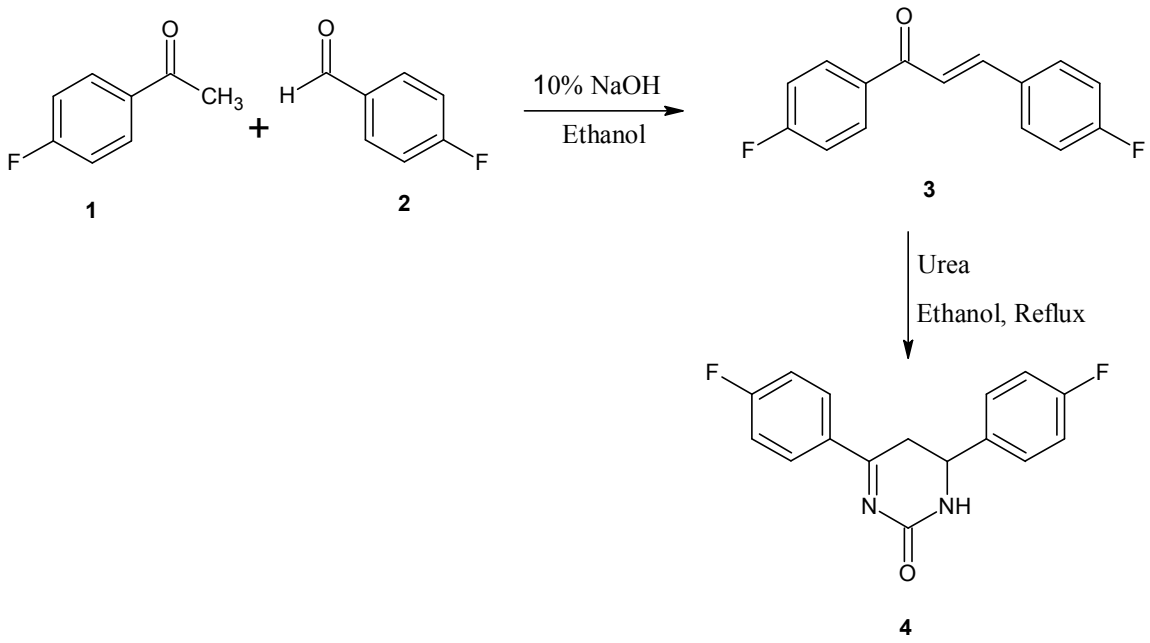

Scheme 1. Synthesis of 4,6-bis(4-fluorophenyl)-5,6-dihydropyrimidin-2(1H)-one

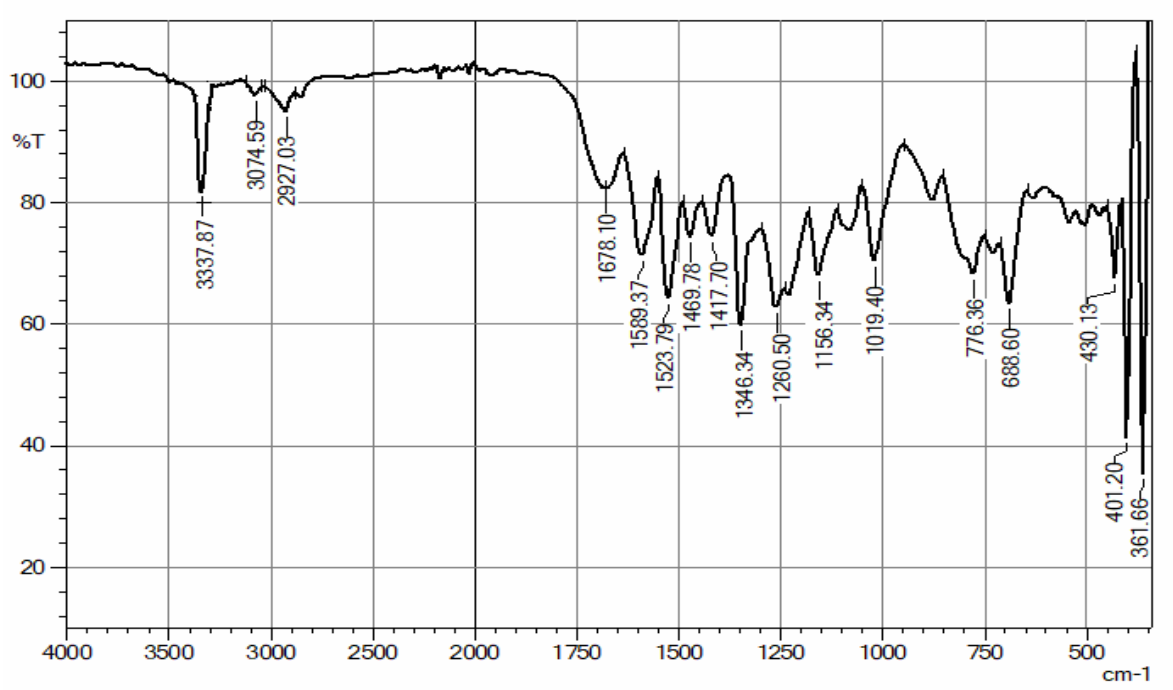

Fig. 2. Experimental FT-IR spectrum of title compound.

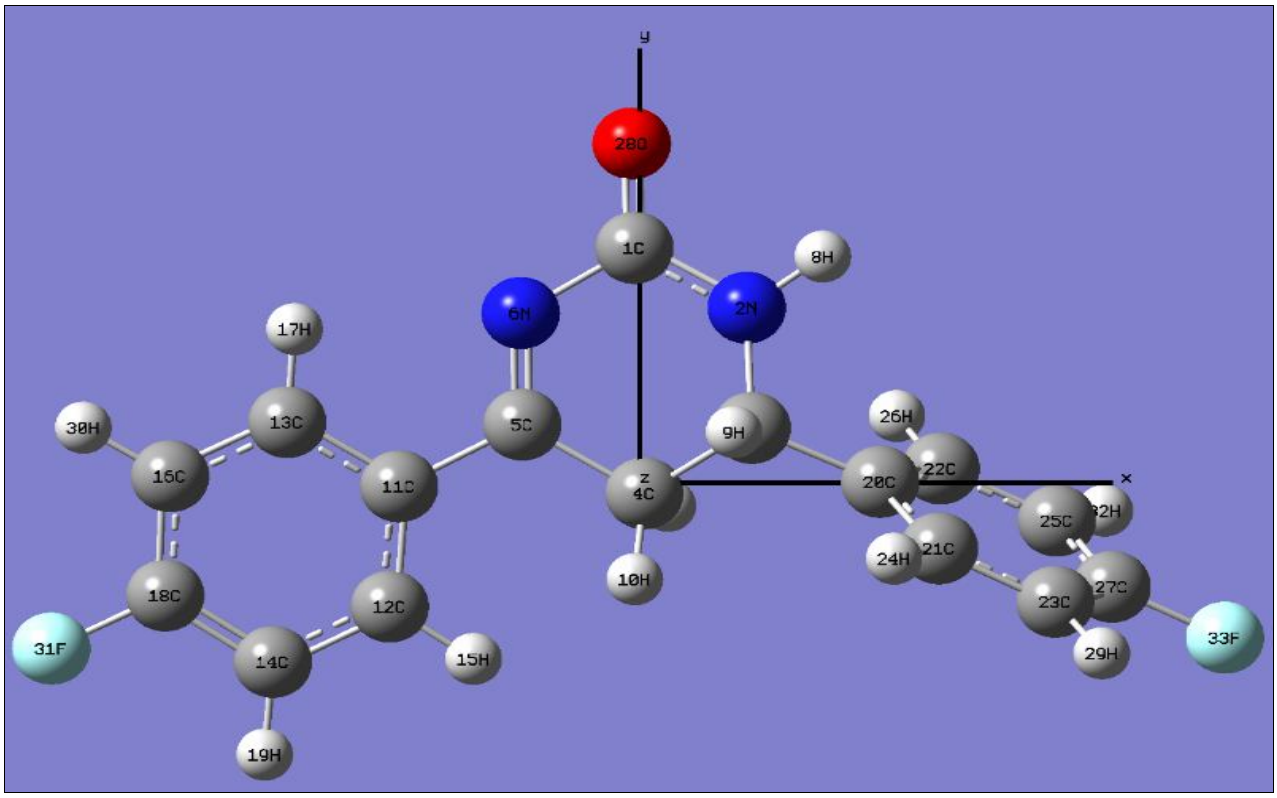

Fig. 3. Optimized structure of the title molecule with atomic labeling in gas phase.

RESULTS AND DISCUSSION

Optimized Geometry and Thermochemical Study

The title compound, 4,6-bis(4-fluorophenyl)-5,6-dihydropyrimidin-2(1H)-one, is composed of three six-member rings. The geometry of this compound was optimized in gas, water and CCl_4 phase by DFT method at B3LYP level with 6-311++G(d,p) basis set. Geometry optimization is the procedure that attempts to find the configuration of minimum energy of the molecule. The procedure calculates the wave function and the energy at a starting geometry and then proceeds to search a new geometry of a lower energy. This is repeated until the lowest energy geometry is found. Geometry optimization calculates the force on each atom by evaluating the gradient of the energy with respect to atomic positions. At last, in minimum energy geometry, the force on each atom is zero. It is worth noting that this procedure will not necessarily find the global minimum. Automatically a sequential search for a minimum finds a local minimum but not necessarily the lowest. The optimization process stops when it finds a stationary point, *i.e.* a point where forces on the atoms are zero. The stationary points and stability of the optimized structures were verified by frequency analysis. The imaginary (negative) frequencies indicate the instability of molecular geometry or in other words, saddle points on the potential energy surface. The geometry of title compound in different media was also characterized by frequency analysis. The most stable point on the potential energy surface was verified by the absence of imaginary frequency.

The optimized structure shows that the title molecule has a non-planar geometry with C1 point group symmetry. The optimized structure in gas phase with their atomic labelling is shown in Fig. 3. The structural parameters like bond lengths, bond angels and dihedral angels provide the essential information about the shape, structure and

molecular conformation of compound. The C3-C4, C4-C5, C3-C20 and C5-C11 bonds have the single bond character and exhibit the bond lengths similar with normal C-C single bond (1.54 Å). The bond lengths of both 4-fluoro phenyl ring carbons are in resemblance with normal bond lengths of aromatic carbons (1.40 Å). The C3 and C4 atoms are sp^3 hybridised while rest of all carbons in molecule are sp^2 hybridized, thereof the bond angles of C4-C3-C20 (112.49°) and C3-C4-C5 (110.16°) show analogy with normal sp^3 bond angle (109.5°). The dihedral angle is a crucial factor to define conformation around rotatable bonds in molecule. Its value ranges from -180 to +180 degrees. The dihedral angles having the range 0 to ±30° indicate the *syn*-conformation and the angles between ±150 to ±180° represent the energetically stable *anti*-conformation of relevant bond. All the bond lengths, bond angles and dihedral angles are compatible with normal values. The structural parameters, bond lengths and bond angles calculated in gas phase from optimized geometry of molecule are presented in Table 1 while dihedral angles are in Table 2. The thermochemical parameters like total thermal energy (E), total molar capacity at constant volume (Cv), entropy (S), zero-point vibrational energy, rotational constant, total potential energy, dipole moment, *etc.* which impact on the thermodynamic stability of molecule are computed at the B3LYP level with 6-311++G (d,p) basis set, at the room temperature, 298.15 K, and 1 atm pressure. The thermochemical parameters of the title molecule in gas phase are enlisted in Table 3.

Electronic Properties and Absorption Studies

The quantum chemical calculations are important for obtaining information about the electrochemical behaviour of organic compounds. The frontier molecular orbital (FMO) analysis of title compound was performed at the B3LYP/6-311++G(d,p) level. The FMO analysis considers interactions of filled molecular orbitals with empty molecular orbitals. The highest occupied molecular orbital (HOMO) and the lowest unoccupied molecular orbital (LUMO) are the main orbitals taking part in chemical stability of compounds. HOMO acts as an electron donor and LUMO as an electron acceptor. The difference between the energies of HOMO and LUMO is referred as energy gap which determines the reactivity and kinetic stability of molecules. Hard molecules have a high energy gap and soft molecules have a small energy gap. The HOMO-LUMO energy gap (ΔE) of title compound is found to be 3.3587, 3.3609 and 3.3571 eV in gas, water and CCl_4, respectively, which explains the eventual charge transfer interactions taking place within the molecule. The pictorial representation of the frontier molecular orbitals in gas phase is shown in Fig. 4.

The global reactivity descriptors such as electronegativity (χ), chemical hardness (η), chemical softness (S), chemical potential (μ), global electrophilicity index (ω) and maximum number of electrons transferred (ΔNmax) are promising DFT descriptors to identify the chemical reactivity of molecules. The global reactivity descriptors of title molecule were calculated using Koopmans theorem [29,30]. Global chemical reactivity descriptors and HOMO-LUMO energies in gas, water and CCl_4 are listed in Table 4. Energy gap (ΔE) and reactivity descriptors of the molecule almost do not change in the gas phase, as well as in water and CCl_4 solvents. The calculated values of the electronegativity for the title molecule are found to be quite high, 7.9463, 7.9526 and 7.9477 eV in gas, water and CCl_4, respectively, which is attributed to the presence of two fluorine atoms in molecule. The lower softness value in all media indicates less polarizability of molecule. The absorption energy, excitation energy, oscillator strength and transitions of title compound computed at TD-B3LYP/6-311++G(d,p) level of theory for B3LYP/6-311++G(d,p) optimized geometry in gas phase are given in Table 5. The maximum absorption of molecule (331.88 nm) is because of the less energetic transition of electron from HOMO to LUMO (H-- > L). The excitation energy for the excitation of electron from ground state to excited state-1 (S0-- > S1) is 3.7358 eV.

Mullikan Atomic Charges

The Mulliken atomic charges in molecule are fundamental and an expedient tool to interpret the properties of compounds with their structure. The atomic charges in molecule serve to provide a simple picture of the electron density distribution over the molecule. The net charge on the studied molecule is zero. The Mulliken atomic charges of the title molecule calculated in the gas phase at B3LYP level with 6-311++G(d,p) basis set are listed in Table 6. The

Table 1. Optimized Bond Lengths and Bond Angles Calculated at the B3LYP/6-311++G(d,p) Level

Bond lengths (Å)					
C1-N2	1.3793	C5-C11	1.4843	C20-C21	1.3972
C1-N6	1.4193	C11-C12	1.4030	C20-C22	1.3999
C1-O28	1.2142	C11-C13	1.4069	C21-C23	1.3940
N2-C3	1.4584	C12-C14	1.3922	C21-H24	1.0851
N2-H8	1.011	C12-H15	1.0822	C22-C25	1.3920
C3-C4	1.5348	C13-C16	1.3862	C22-H26	1.0840
C3-H9	1.1002	C13-H17	1.0822	C23-C27	1.3849
C3-C20	1.5175	C14-C18	1.3850	C23-H29	1.0827
C4-C5	1.5182	C14-H19	1.0826	C25-C27	1.3870
C4-H7	1.0967	C16-C18	1.3894	C25-H32	1.0829
C4-H10	1.0898	C16-H30	1.0828	C27-F33	1.3541
C5-N6	1.2861	C18-F31	1.3509	-	-
Bond angles (°)					
N2-C1-N6	117.55	N6-C5-C11	117.81	C3-C20-C21	120.06
N2-C1-O28	121.88	C1-N6-C5	120.98	C3-C20-C22	121.17
N6-C1-O28	120.56	C5-C11-C12	122.34	C21-C20-C22	118.75
C1-N2-C3	122.37	C5-C11-C13	119.18	C20-C21-C23	121.16
C1-N2-H8	114.23	C12-C11-C13	118.47	C20-C21-H24	119.69
C3-N2-H8	118.35	C11-C12-H14	121.11	C23-C21-H24	119.14
N2-C3-C4	107.11	C11-C12-H15	120.07	C20-C22-C25	120.91
N2-C3-H9	110.17	C14-C12-H15	118.09	C20-C22-H26	119.73
N2-C3-C20	111.48	C11-C13-C16	121.07	C25-C22-H26	119.34
C4-C3-H9	107.79	C11-C13-H17	118.29	C21-C23-C27	118.35
C4-C3-C20	112.49	C16-C13-H17	120.63	C21-C23-H29	121.72
H9-C3-C20	107.73	C12-C14-C18	118.44	C27-C23-H29	119.92
C3-C4-C5	110.16	C12-C14-H19	121.66	C22-C25-C27	118.57
C3-C4-H7	109.87	C18-C14-H19	119.89	C22-C25-H32	121.64
C3-C4-H10	109.06	C13-C16-C18	118.56	C27-C25-H32	119.78
C5-C4-H7	108.83	C13-C16-H30	121.66	C27-C27-C25	122.24
C5-C4-H10	111.56	C18-C16-H30	119.76	C23-C27-F33	118.92
H7-C4-H10	107.30	C14-C18-C16	122.33	C25-C27-F33	118.83
C4-C5-N6	122.34	C14-C18-F31	118.84	-	-
C4-C5-C11	119.84	C16-C18-F31	118.83	-	-

Table 2. Optimized Dihedral Angles Calculated at B3LYP/6-311++G(d,p) Level

Dihedral angles (°)					
N6-C1-N2-C3	-12.89	H7-C4-C5-N6	-90.99	H19-C14-C18-F31	0.27
N6-C1-N2-H8	-167.3	H7-C4-C5-C11	87.97	C13-C16-C18-C14	0.04
O28-C1-N2-C3	167.9	H10-C4-C5-N6	150.8	C13-C16-C18-F31	-179.8
O28-C1-N2-H8	13.52	H10-C4-C5-C11	-30.23	H30-C16-C18-C14	179.7
N2-C1-N6-C5	-12.31	C4-C5-N6-C1	2.04	H30-C16-C18-F31	-0.11
O28-C1-N6-C5	166.8	C11-C5-N6-C1	-176.1	C3-C20-C21-C23	178.0
C1-N2-C3-C4	42.62	C4-C5-C11-C12	-5.07	C3-C20-C21-H24	-2.29
C1-N2-C3-H9	-74.35	C4-C5-C11-C13	176.1	C22-C20-C21-C23	-0.52
C1-N2-C3-C20	166.0	N6-C5-C11-C12	173.9	C22-C20-C21-H24	179.1
H8-N2-C3-C4	-163.9	N6-C5-C11-C13	-4.85	C3-C20-C22-C25	-178.2
H8-N2-C3-H9	79.08	C5-C11-C12-C14	-178.9	C3-C20-C22-H26	2.40
H8-N2-C3-C20	-40.47	C5-C11-C12-H15	0.30	C21-C20-C22-C25	0.26
N2-C3-C4-C5	-47.42	C13-C11-C12-C14	-0.14	C21-C20-C22-H26	-179.0
N2-C3-C4-H7	72.46	C13-C11-C12-H15	179.1	C20-C21-C23-C27	0.33
N2-C3-C4-H10	-170.1	C5-C11-C13-C16	179.5	C20-C21-C32-H29	179.8
H9-C3-C4-C5	71.11	C5-C11-C13-H17	-0.32	H24-C21-C23-C27	-179.3
H9-C3-C4-H7	-168.9	C12-C11-C13-C16	0.67	H24-C21-C23-H29	0.13
H9-C3-C4-H10	-51.64	C12-C11-C13-H17	-179.1	C20-C22-C25-C27	0.15
C20-C3-C4-C5	-170.2	C11-C12-C14-C18	-0.40	C20-C22-C25-H32	-179.6
C20-C3-C4-H7	-50.37	C11-C12-C14-H19	179.6	H26-C22-C25-C27	179.4
C20-C3-C4-H10	66.97	H15-C12-C14-C18	-179.6	H26-C22-C25-H32	-0.35
N2-C3-C20-C21	135.5	H15-C12-C14-H19	0.37	C21-C23-C27-C25	0.10
N2-C3-C20-C22	-45.92	C11-C13-C16-C18	-0.62	C21-C23-C27-F33	179.7
C4-C3-C20-C21	-104.0	C11-C13-C16-H30	179.6	H29-C23-C27-C25	-179.3
C4-C3-C20-C22	74.41	H17-C13-C16-C18	179.1	H29-C23-C27-F33	0.24
H9-C3-C20-C21	14.57	H17-C13-C16-H30	-0.51	C22-C25-C27-C23	-0.34
H9-C3-C20-C22	-166.9	C12-C14-C18-C16	0.46	C22-C25-C27-F33	-179.9
C3-C4-C5-N6	29.52	C12-C14-C18-F31	-179.6	H32-C25-C27-C23	179.5
C3-C4-C5-C11	-151.5	H19-C14-C18-C16	-179.6	H32-C25-C27-F33	-0.12

Table 3. Thermochemical Parameters Calculated in Gas Phase at the B3LYP/6-311++G(d,p) Level

Parameters	Values
Total E Thermal kcal mol^{-1}	166.761
Translational	0.889
Rotational	0.889
Vibrational	164.983
Total Molar capacity at constant volume (Cv) Cal mol^{-1} $Kelvin^{-1}$	65.732
Translational	2.981
Rotational	2.981
Vibrational	59.770
Total entropy (S) Cal mol^{-1} $Kelvin^{-1}$	136.707
Translational	42.851
Rotational	34.927
Vibrational	58.929
Zero-point vibrational energy (kcal mol^{-1})	156.20680
Rotational Constant (GHz)	0.58934
	0.12751
	0.10905
E (RB3LYP) (a.u.)	-1001.62167907
Dipole moment (Debye)	4.8580

C20 atom possesses more positive charge while both nitrogen atoms of pyrimidinone ring and both fluorine atoms have a negative charge. All hydrogens are possessing positive charge. The graphical illustration of Mulliken charges in gas phase is displayed in Fig. 5.

Molecular Electrostatic Potential

Molecular electrostatic potential (MEP) elucidates the charge distribution of molecules in three dimensions. The charge distribution within molecule helps explain the reactivity of molecule. In the MEP map, the electrostatic potential at the surface of molecule is represented by distinct colours. The red and yellow colour represents the negative electrostatic potential and prone to electrophilic attack while blue colour represents the positive electrostatic potential and responsible for nucleophilic reactivity. The green color represents the region of zero potential. MEP for title molecule was plotted in gas phase at the B3LYP/6-311++G(d,p) level is shown in Fig. 6. In title molecule, the carbonyl oxygen has the most negative electrostatic potential, while C=N has the positive potential and is considered as a site for nucleophilic attack. The electrostatic potential is also represented by using electrostatic potential counters as shown in Fig. 7. The denser area in MEP's

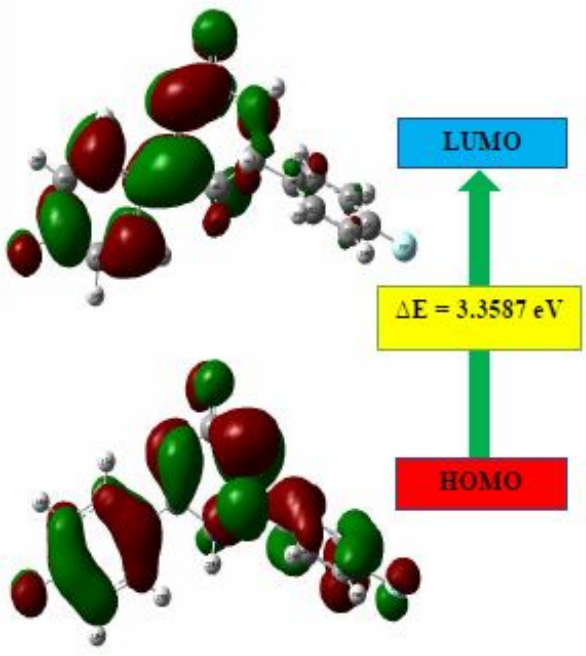

Fig. 4. Frontier molecular orbitals of title molecule in gas phase.

Table 4. The Global Chemical Reactivity Descriptors of the Title Molecule

Molecular properties	Value		
	Gas	Water	CCl_4
E_{HOMO}	-9.6257 eV	-9.6331 eV	-9.6263 eV
E_{LUMO}	-6.2670 eV	-6.2722 eV	-6.2692 eV
ΔE (E_{LUMO}-E_{HOMO})	3.3587 eV	3.3609 eV	3.3571 eV
Ionisation energy (I)	9.6257 eV	9.6331 eV	9.6263 eV
Electron affinity (EA)	6.2670 eV	6.2722 eV	6.2692 eV
Electronegativity (χ)	7.9463 eV	7.9526 eV	7.9477 eV
Chemical hardness (η)	1.6793 eV	1.6804 eV	1.6785 eV
Chemical softness (S)	0.5955 eV^{-1}	0.5951 eV^{-1}	0.5958 eV^{-1}
Chemical potential (μ)	-7.9463 eV	-7.9526 eV	-7.9477 eV
Global electrophilicity index (ω)	18.8005 eV	18.8181 eV	18.8162 eV
Maximum number of electrons transferred (ΔN_{max})	4.7319 eV	4.7326 eV	4.7350 eV

Table 5. Absorption Energy (λ in nm), Excitation Energy (in eV), Oscillator Strength (*f*) and Transitions of the Studied Molecule in Gas Phase

State	λ^{abs}	Excitation energy	*f*	Transition orbitals	Transition
S0-- > S1	331.88	3.7358	0.0015	74 - > 75	H-- > L

Table 6. Mulliken Atomic Charges in Gas Phase

Atom	Charge	Atom	Charge	Atom	Charge
C1	0.2470	C12	-0.3330	C23	0.1769
N2	-0.3183	C13	-0.1577	H24	0.1559
C3	0.3093	C14	-0.3705	C25	0.1009
C4	-1.1201	H15	0.1511	H26	0.2013
C5	-0.1041	C16	-0.2019	C27	-0.7025
N6	-0.0264	H17	0.2405	O28	-0.2880
H7	0.2136	C18	-0.4009	H29	0.2108
H8	0.3365	H19	0.1986	H30	0.2064
H9	0.2538	C20	1.0037	F31	-0.1679
H10	0.1296	C21	-0.5923	H32	0.2111
C11	1.0720	C22	-0.4705	F33	-0.1649

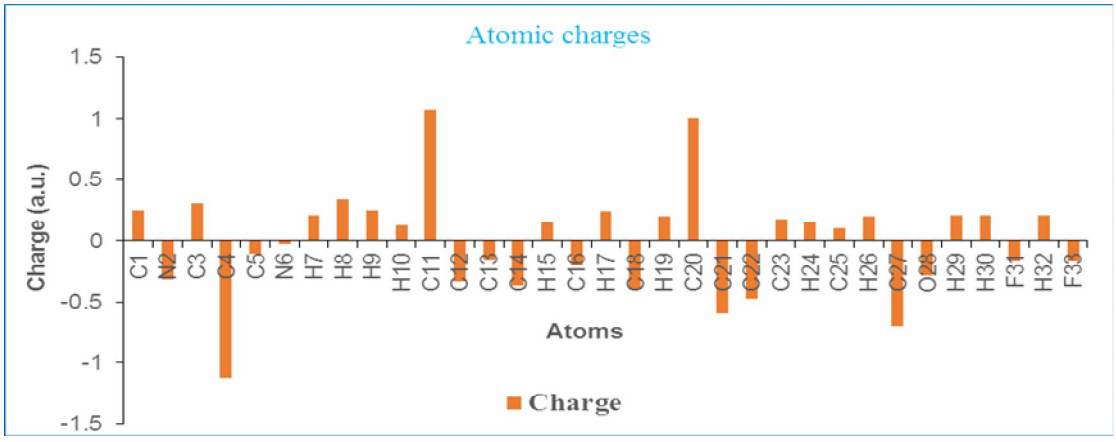

Fig. 5. The atomic charge plot of the target molecule.

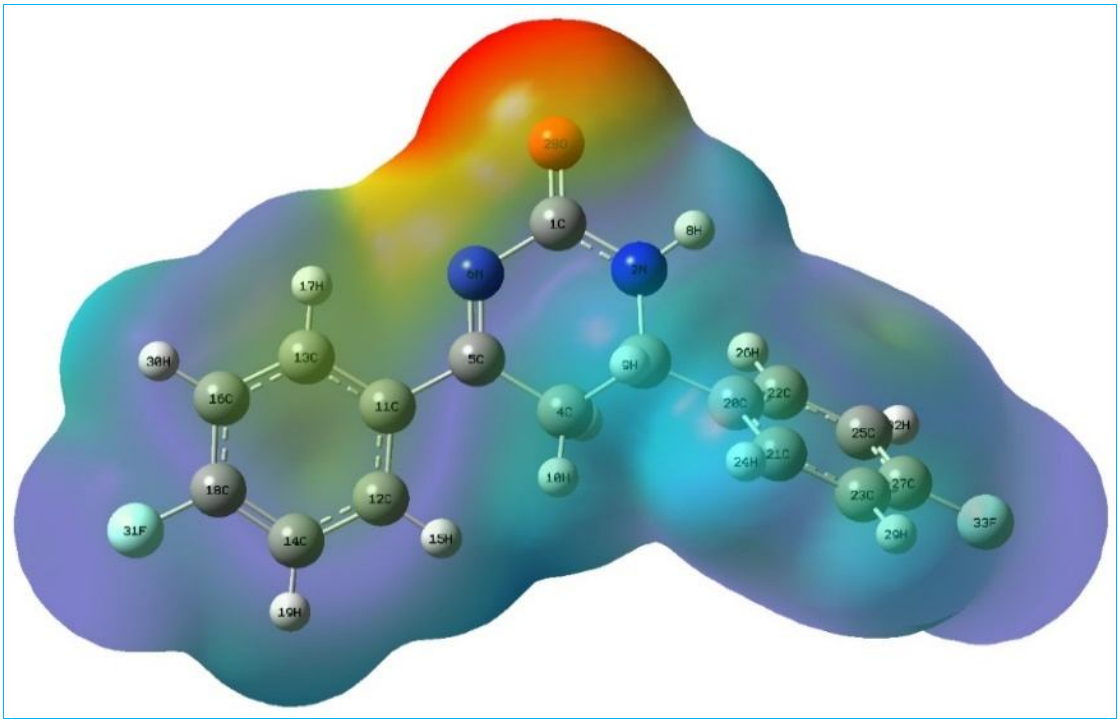

Fig. 6. MEP surface diagram of title molecule in gas phase.

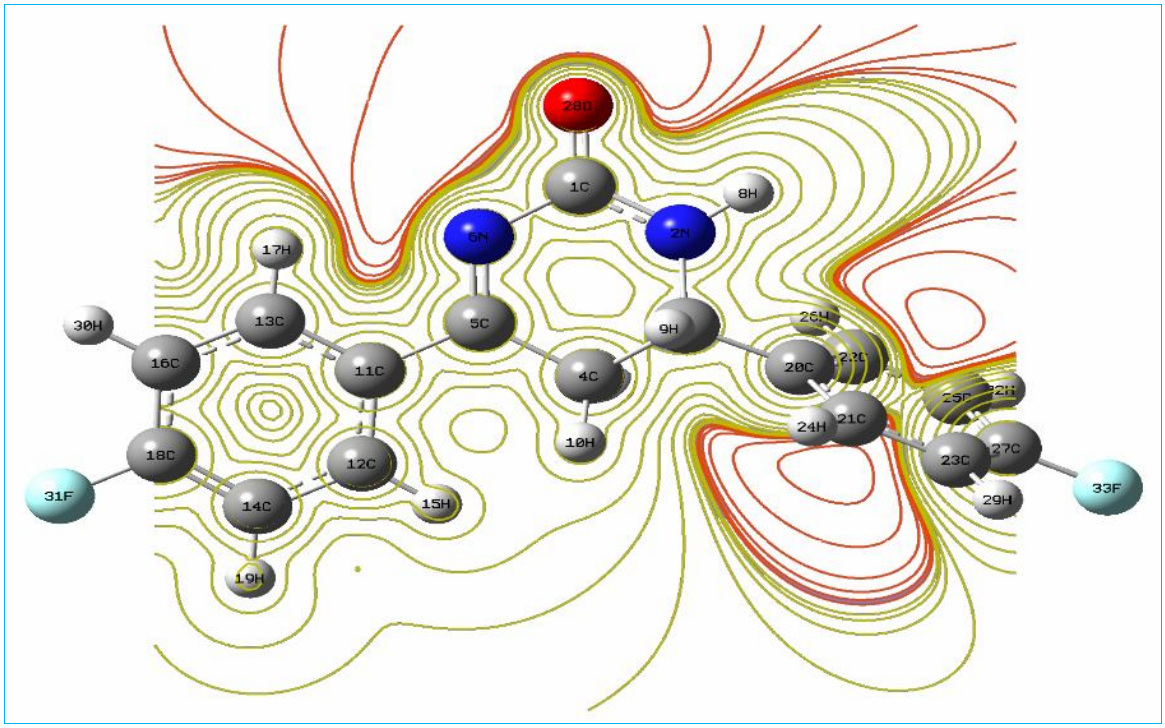

Fig. 7. Electrostatic potential counter plot of the title molecule.

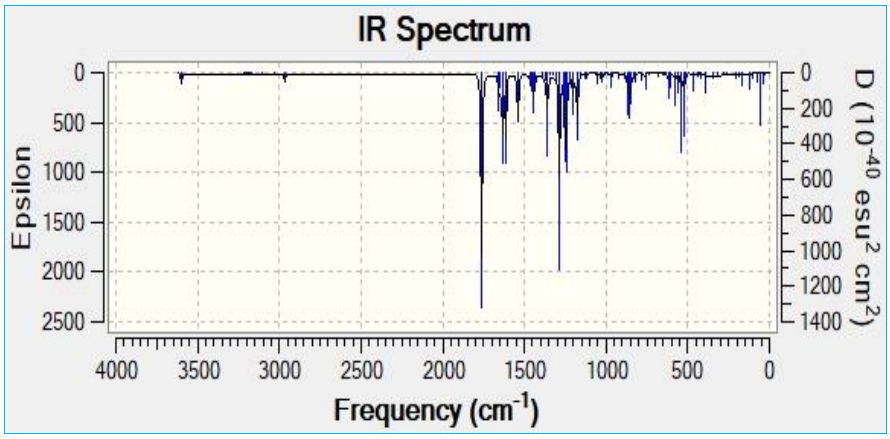

Fig. 8. Computed IR spectrum of studied compound in gas phase.

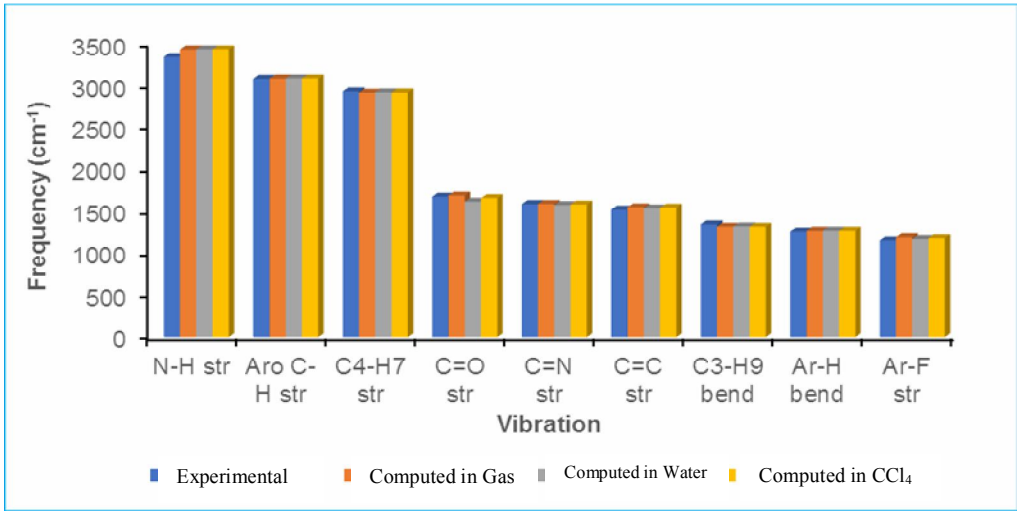

Fig. 9. Correlation graphics of computed and experimental frequencies.

contour lines represents the stronger electrostatic field than the region with less contour lines. The red region in counter map of the compound represents higher electron density, which favours the approach of electrophilic species and repel of the nucleophilic ones.

Vibrational Analysis

The experimental FT-IR spectrum of title compound was recorded in the solid phase (Fig. 2) while vibrational spectra are computed in the gas phase, water and CCl_4 solvents at B3LYP/6-311++G(d,p) level. The computed IR spectrum of the compound in gas phase is depicted in Fig. 8. The target molecule has 33 total number of atoms. Because of the non-planar structure, it has 93 fundamental mode of vibrations according to 3N-6 formula. The theoretically predicted vibrational frequencies are scaled by an empirical factor 0.9613 [31]. The comparative studies of the selected experimental and computed vibrational frequencies in gas phase, water and CCl_4 solvents are noted in Table 7. Figure 9 elucidates the correlation between experimental and computed frequencies graphically. The results of vibrational analysis confirms that frequencies calculated in

Table 7. Selected Experimental and Computed Vibrational Assignments of the title Molecule

Mode	Computed scaled frequencies (cm^{-1})			IR Intensity (km) mol^{-1}	Experimental frequencies	Assignment
	Gas	Water	CCl_4	(gas phase)	(cm^{-1})	
93	3428	3429	3430	33.73	3337	N-H str
92	3088	3090	3089	5.51	-	C13-H17, C16-H30 str
89	3077	3078	3078	1.47	3074	C25-H32, C22-H26 str
87	3068	3075	3072	5.86	-	C12-H15, C14-H19 str
84	2988	3002	2995	8.46	-	C4-H10 str
83	2912	2916	2914	6.78	2927	C4-H7 str
82	2851	2877	2864	30.27	-	C3-H9 str
81	1692	1618	1661	582.47	1678	C=O str
80	1591	1578	1585	88.96	1589	C=N str
76	1551	1538	1546	207.32	1523	Ring A aro C=C str
75	1480	1473	1476	206.74	-	Ring B aro C=C str
68	1317	1320	1316	13.69	1346	C3-H9 ip bend
65	1272	1273	1272	3.77	-	Ring B Ar-H ip bend
64	1269	1271	1270	3.30	1260	Ring A Ar-H ip bend
62	1234	1256	1244	356.10	-	C1-N2 str
59	1195	1174	1184	173.02	1156	Ar-F str

str: stretching; ip bend: in plane bending; aro: aromatic; Ar: aryl; Ring A: 4-fluorophenyl ring attached to C5; Ring B: 4-fluorophenyl ring attached to C3.

gas phase by DFT with B3LYP/6-311++G(d,p) level show a good coherence with experimental frequencies.

N-H Vibrations

The N-H stretching vibrations normally appear in the spectral region of middle IR at 3300-3500 cm^{-1} [32,33]. Experimentally the N-H stretching frequency for the target molecule is observed at 3337 cm^{-1}, and computed N-H stretching modes of vibration appear at 3428, 3429 and 3430 cm^{-1} in gas phase, water and CCl_4 solvents, respectively.

C-H Vibrations

The aromatic C-H stretching vibrations are expected in the region 3000-3100 cm^{-1} while aliphatic C-H stretching vibrations appear in the range 2850-3000 cm^{-1} [32,33]. In the title molecule, the calculated values of C-H stretching modes appear at 3088, 3077, 3068, 2988, 2912 and 2851 cm^{-1} in gas phase, which are also not much different in water and CCl_4 solvents (Table 7). Experimentally the peaks at 3074 and 2927 cm^{-1} are observed in the IR spectrum of the title molecule due to C-H stretching vibrations. The C-H bending vibrations normally appear in the region 1250-

1400 cm^{-1}. The computed C-H bending modes of vibration appear at 1269 and 1317 cm^{-1} in gas phase while experimentally C-H bending frequencies are seen at 1260 and 1346 cm^{-1}.

C=O Vibrations

If compound contains carbonyl group, then absorption caused by C=O stretching is very important. All carbonyl compounds possess an intense peak in the region 1650-1820 cm^{-1}. The C=O stretching vibrational frequency in amides is affected by electron donating resonance of adjacent lone pair present on nitrogen and normally appears in the spectral region 1630-1690 cm^{-1}. In the experimental FT-IR spectrum of the target compound, the peak at 1678 cm^{-1} is due to the C=O stretching vibration while DFT calculations show this stretching mode of vibration at 1692 cm^{-1} in gas phase, 1618 cm^{-1} in water and 1661 cm^{-1} in CCl_4 solvent. The results reveal that C=O stretching frequency is decreased in water phase, because water forms the intermolecular hydrogen bonding with carbonyl oxygen which weakens the carbonyl bond. The non polar solvent CCl_4 does not produce such type of effect, so C=O stretching frequency remains unaffected in CCl_4.

Ar-F Vibrations

Generally, Ar-F stretching frequency appears in the region of 1100-1270 cm^{-1}. In the experimental FT-IR spectrum of the molecule under study, the Ar-F stretching vibration is observed at 1156 cm^{-1} while DFT calculations give Ar-F stretching mode at 1195, 1174 and 1184 cm^{-1} in gas phase, water and CCl_4 solvents, respectively.

CONCLUSIONS

The 4,6-bis(4-fluorophenyl)-5,6-dihydropyrimidin-2(1*H*)-one molecule was synthesized and characterized using FT-IR and ^{1}H NMR spectroscopies. To establish the molecular structure of the synthesized compound the quantum chemical calculations were performed by density functional theory at the B3LYP level with 6-311++G(d,p) basis set in gas phase, water and CCl_4 solvents. The HOMO-LUMO and global chemical reactivity descriptors revealed that there is no remarkable difference for energy gap (ΔE) and other reactivity descriptor values in gas, water and CCl_4 phases. The lower value of frontier orbital energy gap and the higher value of the dipole moment imply the higher reactivity of title molecule. The MEP analysis demonstrates the distribution of electron density across the molecule. The MEP plot indicates that electropositive region is mainly located over the C=N group of pyrimidinone ring which is considered as the site for nucleophilic attack, while the electronegative region is mostly located over the carbonyl oxygen which is considered as the site for electrophilic attack. The comparison between the computed and experimental data indicates that the calculated vibrational frequencies in gas phase at the B3LYP/6-311++G(d,p) level are in a good agreement with the experimental values. Because of the hydrogen bonding, carbonyl stretching frequency appears at least value in polar protic solvent water while the rest of frequencies are not much affected by solvents. The calculated frequencies in gas phase and non-polar solvent CCl_4 are not differentiated in a large amount. Overall, the results predominantly clarify that the DFT-based structural parameters, electronic properties, thermodynamic functions and reactivity descriptors are used for illustration of the favoured reactive sites and provide a firm explanation for the reactivity of the molecule under study.

ACKNOWLEDGEMENTS

Authors are thankful to DST-FIST New Delhi for providing instrumental grant for research to the M.S.G. College Malegaon. Authors acknowledge the Central Instrumentation Facility (CIF), Savitribai Phule Pune University, Pune for spectral analysis. Authors are also grateful to Ex Professor A. B. Sawant for Gaussian study. Dr. Apoorva Hiray, Coordinator, M. G. Vidyamandir institute, is gratefully acknowledged for Gaussian package.

REFERENCES

[1] Sondhi, S. M.; Singh, N.; Johar, M.; Kumar, A., Synthesis, anti-inflammatory and analgesic activities evaluation of some mono, bi and tricyclic pyrimidine derivatives. *Bioorg. Med. Chem.* **2005**, *13*, 6158-6166, DOI: 10.1016/j.bmc.2005.06.063.

[2] Alam, O.; Khan, S. A.; Siddiqui, N.; Ahsan, W.;

Verma, S. P.; Gilani, S. J., Antihypertensive activity of newer 1,4-dihydro-5-pyrimidine carboxamides: Synthesis and pharmacological evaluation. *Eur. J. Med. Chem.* **2010**, *45*, 5113-5119, DOI: 10.1016/j.ejmech.2010.08022.

[3] Cordeu, L.; Cubedo, E.; Bandres, E.; Rebollo, A.; Saenz, X.; Chozas, H.; Dominguez, M. V.; Echeverria, M.; Mendivil, B.; Sanmartin, C. *et al.*, Biological profile of new apoptotic agents based on 2,4-pyrido[2,3-d]pyrimidine derivatives. *Bioorg. Med. Chem.* **2007**, *15*, 1659-1669, DOI: 10.1016/j.bmc.2006.12.010.

[4] Tokutake, N., Brit. Pat. 146836B in *Chem. Abstr.* **1977**, *87*, 102370.

[5] Johar, M.; Manning, T.; Kunimoto, D. Y.; Kumar, R., Synthesis and *in vitro* anti-mycobacterial activity of 5-substituted pyrimidine nucleosides. *Bioorg. Med. Chem.* **2005**, *13*, 6663-6671, DOI: 10.1016/j.bmc.2005.07.046.

[6] Cosimelli, B; Greco, G.; Ehlardo, M.; Novellino, E., *et al.*, Derivatives of 4-amino-6-hydroxy-2-mercaptopyrimidine as novel, potent, and selective A3 adenosine receptor antagonists. *J. Med. Chem.* **2008**, *51*, 1764-1770, DOI: 10.1021/jm701159t.

[7] Li, J.; Zhao, Y. F.; Zhao, X. L.; Yuan, X. Y.; Gong, P., Synthesis and anti-tumor activities of novel pyrazolo[1,5-a]pyrimidines. *Arch. Pharm. Chem. Life Sci.* **2006**, *339*, 593-597, DOI: 10.1002/ardp.200600098.

[8] Shallal, H. M.; Russu, W. A., Discovery, synthesis and investigation of the antitumor activity of novel piperazinylpyrimidine derivatives. *Eur. J. Med. Chem.* **2011**, *46*, 2043-2057, DOI: 10.1016/j.ejmech.2011.02.057.

[9] Rostom, S. A.; Badr, M. H.; Abd El Razik, H. A.; Ashour, H. M.; Abdel Wahab, A. E., Synthesis of some pyrazolines and pyrimidines derived from polymethoxy chalcones as anticancer and antimicrobial agents. *Archiv der Pharmazie,* **2011**, *344*, 572-587, DOI: 10.1002/ardp.201100077.

[10] Trivedi, A. R.; Dodiya, D. K.; Ravat, N. R.; Shah, V. R., Synthesis and biological evaluation of some new pyrimidines *via* a novel chalcone series. *ARKIVOC,* **2008**, *XI*, 131-141, DOI: 10.3998/ark.5550190.0009.b13.

[11] Umaa, K.; Ramanathan, M.; Krishnakumar, K.; Kannan, K., Elucidation and evaluation of substituted pyrimidines. *Asian J. Chem.,* **2009**, *21*, 6674-6678.

[12] Umesha, B.; Sowbhagya; Basavaraju, Y. B., Synthetic study on chalcone and their dihydropyrimidinone and dihydropyrimidinethione derivatives. *Int. J. Scientific Res. in Science & Tech.* **2016**, *2*, 340-343. DOI: 10.32628/IJSRST162343.

[13] Yokota, K.; Hagimori, M.; Mizuyama, N.; Nishimura, Y.; Fujito, H.; Shigemitsu, Y.; Tominaga, Y., Synthesis, solid-state fluorescence properties and computational analysis of novel 2-aminobenzo[4,5]thieno[3,2-d]pyrimidine-5,5-dioxides. *Beilstein J. Org. Chem.* **2012**, *8*, 266-274, DOI: 10.3762/bjoc.8.28.

[14] Beyramabadi, S. A.; Morsali, A.; Shams, A., N,N'-dipyridoxyl(1,2-diaminocyclohexane) and its Cu(II) complex: Synthesis, experimental and theoretical studies. *J. Struct. Chem.* **2015**, *56*, 243-249, DOI: 10.1134/S0022476612020067.

[15] Santiago, A., A systematic computational study on flavonoids. *Int. J. Mol. Sci.,* **2010**, *11*, 2017-2038, DOI: http://hdl.handle.net/123456789/13299.

[16] Arivazhagan, M.; Prabhakaran, S., DFT studies and vibrational spectra of 2-bromomethyl-4-nitroanisole. *Ind. J. Pure & Appl. Phys.,* **2012**, *50*, 26-33, DOI: 10.3390/ijms11052017.

[17] Govindarasu, K.; Kavitha, E., Structural, vibrational spectroscopic studies and quantum chemical calculations of n-(2,4-dinitrophenyl)-L-alanine methyl ester by density functional theory. *J. Mol. Struct.* **2015**, *1088*, 70-84, DOI: 10.1016/j.molstruc.2015.02.008.

[18] Govindasamy, P.; Gunasekaran, S., Quantum mechanical calculations and spectroscopic (FT-IR, FT-Raman and UV) investigations, molecular orbital, NLO, NBO, NLMO and MESP analysis of 4-[5-(4-methylphenyl)-3-(trifluoromethyl)-1H-pyrazol-1-yl] benzene-1-sulfonamide. *J. Mol. Struct.* **2015**, *1081*, 96-109, DOI: 10.1016/j.molstruc.2014.10.011.

[19] Sundaraganesan, N.; Meganathan, C.; Joshua, B. D.; Mani, P.; Jayaprakash A., Molecular structure and vibrational spectra of 3-chloro-4-fluoro benzonitrile

by *ab initio* HF and density functional method. *Spectrochim. Acta Part A.* **2008**, *71*, 1134-1139, DOI: 10.1016/j.saa.2008.03.019.

[20] Jagdale, B. S.; Pathade, S. S., Synthesis, characterization and theoretical study of 3-(4-bromophenyl)-5-(2,4-dichlorophenyl)-1-phenyl-4,5-dihydro-1H-pyrazole. *J. Applicable Chem.* **2019**, *8*, 12-19.

[21] Yahyaei, S.; Vessally, E.; Hashemi, M. M., Experimental and theoretical studies on a derivative of tetrahydro-1H benzodiazepine. *Phys. Chem. Res.* **2018**, *6*, 505-519, DOI: 10.22036/pcr.2018.114948.1454.

[22] Beyramabadi, S. A.; Morsali, A.; Khoshkholgh, M. J.; Esmaeili, A. A., N,N'-dipyridoxyl Schiff bases: Synthesis, experimental and theoretical characterization. *Spectrochim. Acta Part A,* **2011**, *83*, 467-471, DOI: 10.1016/j.saa.2011.08.067.

[23] Toozandejani, T.; Beyramabadi, S. A.; Chegini, H.; Khashi, M.; Morsali, A.; Pordel, M., Synthesis, experimental and theoretical characterization of a Mn(II) complex of N,N'-dipyridoxyl(1,2-diaminobenzene). *J. Mol. Struct.* **2017**, *1127*, 15-22, DOI: 10.1016/j.molstruc.2016.07.026.

[24] Mansoorinasab, A.; Morsali, A.; Heravi, M. M.; Beyramabadi, S, A., Quantum mechanical study on the noncovalent adsorption of drug gentamicin onto pristine and COOH functionalized carbon nanotubes. *J. Comput. Theor. Nanosci.* **2015**, *12*, 4935-4941, DOI: https://doi.org/10.1166/jctn.2015.4462.

[25] Pathade, S. S.; Jagdale, B. S., Synthesis and DFT based quantum chemical studies of 2-(3-bromophenyl)-4-(4-bromophenyl)-2,3-dihydro-1H-1, 5-benzodiazepine. *J. Adv. Sci. Res.* **2020**, *11*, 87-94.

[26] Frisch, M. J. *et al.* Gaussian 03, Revision E.01, Gaussian, Inc., Wallingford CT, 2004.

[27] Lee, C.; Yang, W.; Parr, R. G., Development of the Colle-Salvetti correlation-energy formula into a functional of the electron density. *Phys. Rev. B.* **1988**, *37*, 785-789, DOI: 10.1103/PhysRevB.37.785.

[28] Becke, A. D., Density-functional thermochemistry. III. The role of exact exchange. *J. Chem. Phys.* **1993**, *98*, 5648-5652, DOI: 10.1063/1.464913.

[29] Koopmans, T., About the assignments of wave functions and eigenvalues to the individual electrons of an atom. *Physica,* **1934**, *1*, 104-113, DOI: 10.1016/S0031-8914(34)90011-2.

[30] Phillips, J. C., Generalized koopmans theorem. *Phys. Rev.,* **1961**, *123*, 420-424, DOI:10.1103/PhysRev.123.

[31] Foresman, J. B.; Frisch, A. E., Exploring chemistry with electronic structure methods (2nd Edn. Gaussian, Inc. Pittsburgh; PA), 1996.

[32] Kalsi, P. S., Spectroscopy of Organic Compounds. New Age International Pvt. Ltd: New Delhi: 2006, p. 648.

[33] Silverstein, R. M.; Bassler, G. C.; Morrill, T. C., Spectrometric Identification of Organic Compounds. John Wiley: New York, 1991, p. 430.